Electronic Supplementary Material (ESI) for Soft Matter.

Supplementary Information

Investigation of the swollen state of Carbopol molecules in non-aqueous solvents through rheological characterization

Simona Migliozzi, Giovanni Meridiano, Panagiota Angeli* and Luca Mazzei*

Department of Chemical Engineering, University College London, Torrington Place, London WC1E 7JE, UK

** Corresponding Authors: l.mazzei@ucl.ac.uk, p.angeli@ucl.ac.uk*

SI-1 Details of sample preconditioning

The trend of the shear stress σ during sample preconditioning is reported below (SI-1.1) for G solutions at 8% wt of Carbopol. During the pre-shear stage, σ maintains a constant value and suddenly relaxes when the shear rate is forced to 0. The stress appears to plateau to a constant value in roughly 200s. The flow curves obtained for the same sample by waiting 10 minutes and 30 minutes after the pre-shear show good superposition between the data acquired.

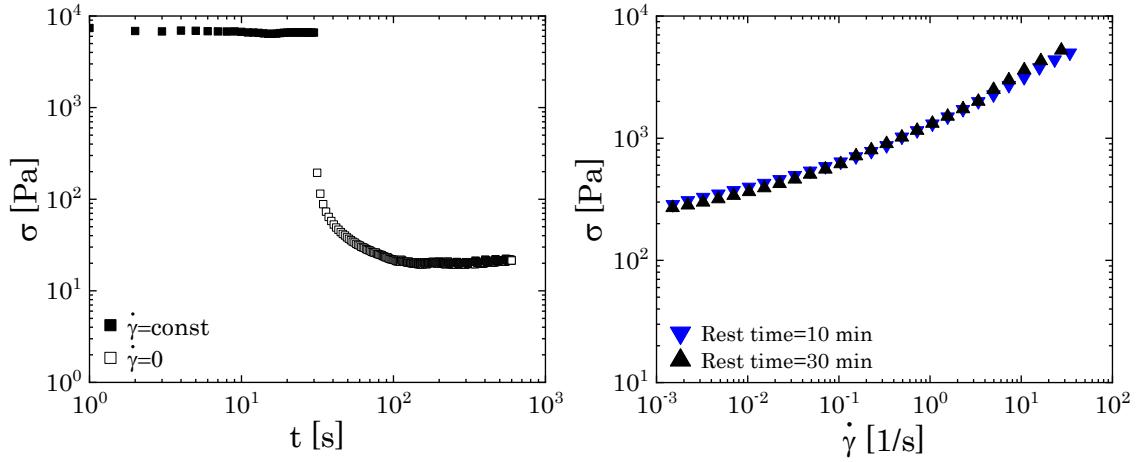

SI-1. 1: (Left) Trend of the shear stress during the pre-shear stage (closed symbols) and during the rest stage (hollow symbols) for G solution at 8% wt of Carbopol; (Right) Steady-shear tests for the same sample concentration with two different resting times.

SI-2 Additional confocal images and summary of all concentrations tested

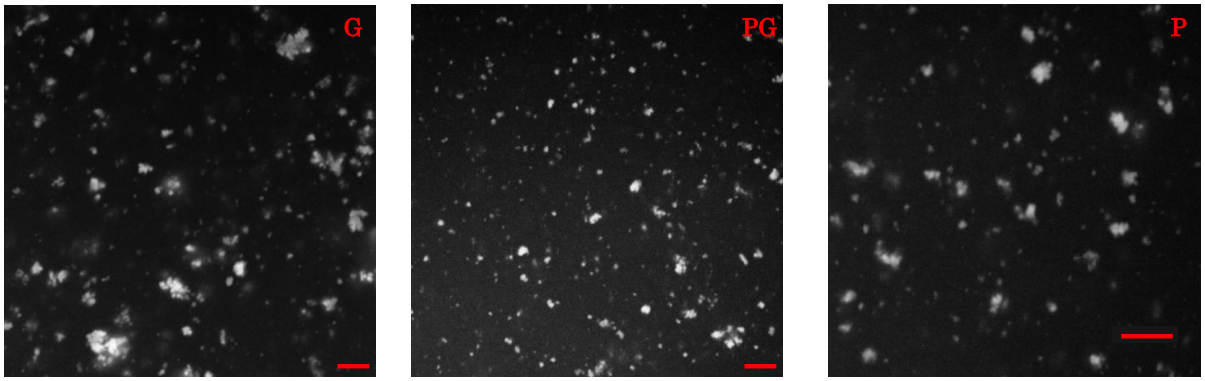

SI-2. 1: Confocal images obtained for G, PG and P solutions at 0.1% wt of Carbopol. The red bar indicates a dimension of 1 μm.

SI-2. 2: Compositions of all samples used in terms of % g/g (w_c), mass concentration (c [g/mL]) and apparent volume fraction ϕ, evaluated from the dimensions obtained through image analysis

	G		PG		P	
w_c (%)	c (g/mL)	ϕ (-)	c (g/mL)	ϕ (-)	c (g/mL)	ϕ (-)
0.15	1.88E-3	0.17	1.78E-3	0.16	1.68E-3	0.092
0.2	2.5E-3	0.23	2.4E-3	0.21	2.24E-3	0.12
0.4	5E-3	0.45	4.75E-3	0.42	4.5E-3	0.25
0.5	6.28E-3	0.56	6E-3	0.52	5.6E-3	0.31
0.55	6.9E-3	0.62	6.54E-3	0.57	6.2E-3	0.34
0.6	7.53E-3	0.68	7.13E-3	0.62	6.73E-3	0.37
0.7	8.8E-3	0.79	8.32E-3	0.73	7.85E-3	0.43
0.8	1E-2	0.90	9.5E-3	0.83	8.97E-3	0.49
0.9	1.13E-2	1.02	1.07E-2	0.94	1E-2	0.56
1	1.25E-2	1.13	1.2e-2	1.04	1.12E-2	0.618
1.5	1.88E-2	1.7	1.78E-2	1.56	1.68E-2	0.927
2	2.5E-2	2.26	2.38E-2	2.09	2.24E-2	1.23
3	3.77E-2	3.4	3.57E-2	3.13	3.37E-2	1.85
5	6.28E-2	5.7	5.94E-2	5.2	5.61E-2	3.09
8	1E-1	9.06	9.5E-2	8.3	8.97E-2	4.9

A rough estimation of the apparent volume fraction ϕ of all the sample can be obtained assuming a linear relation between the mass and volume of the microgel particles:

$$\phi = \frac{1}{\rho_p}\left(\frac{R_{SW}}{R_{IN}}\right)^3 c \qquad (SI\text{-}3.1)$$

where ρ_p is the particle density ($\rho_p = 1.24$ g cm^{-3}) , c is the mass concentration and R_{SW} and R_{IN} are

the radius of the swollen and dry particle, respectively. The results obtained using the dimensions from the analysis of the confocal images are reported above in Table SI-2.2.

SI-3 Derivative of the loss moduli close to the jamming transition and summary of the evolution of G' and G'' with Carbopol concentration

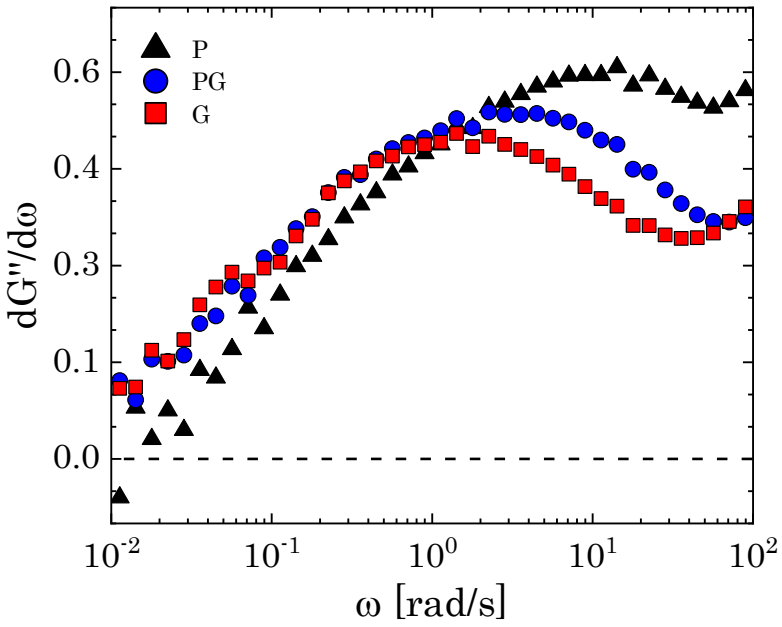

SI-3. 1: First derivative of G'' for all solutions at 2% wt of Carbopol. For all solutions the derivative approaches zero for low values of ω.

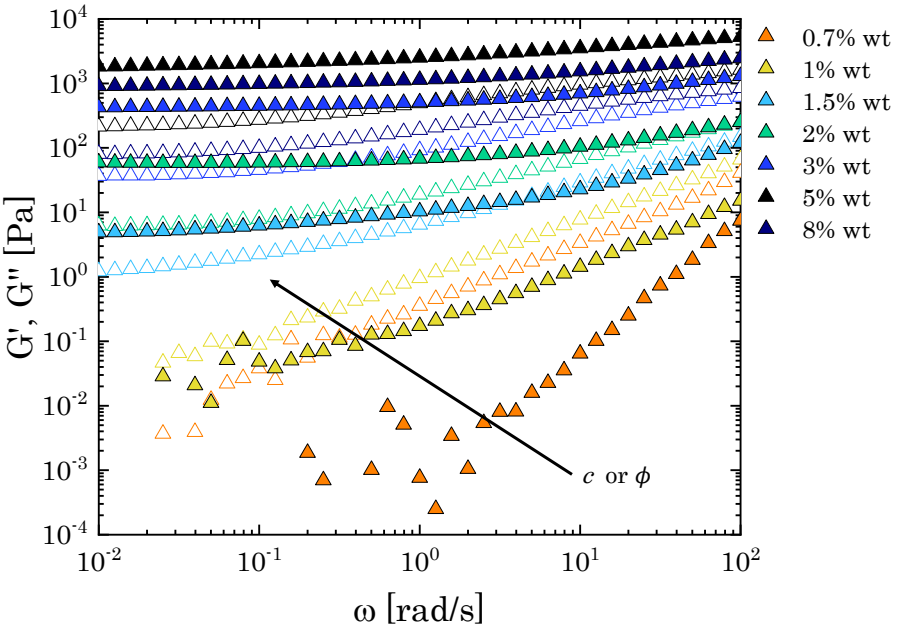

SI-3. 2: Summary of the evolution of the storage (close symbols) and loss (hollow symbols) moduli with the increase of Carbopol concentration. The graph reports the results obtained only for P solutions, but the same evolution is alos observed with the other two solvents.

SI-4 Trend of the loss tangents tanδ with Carbopol concentration

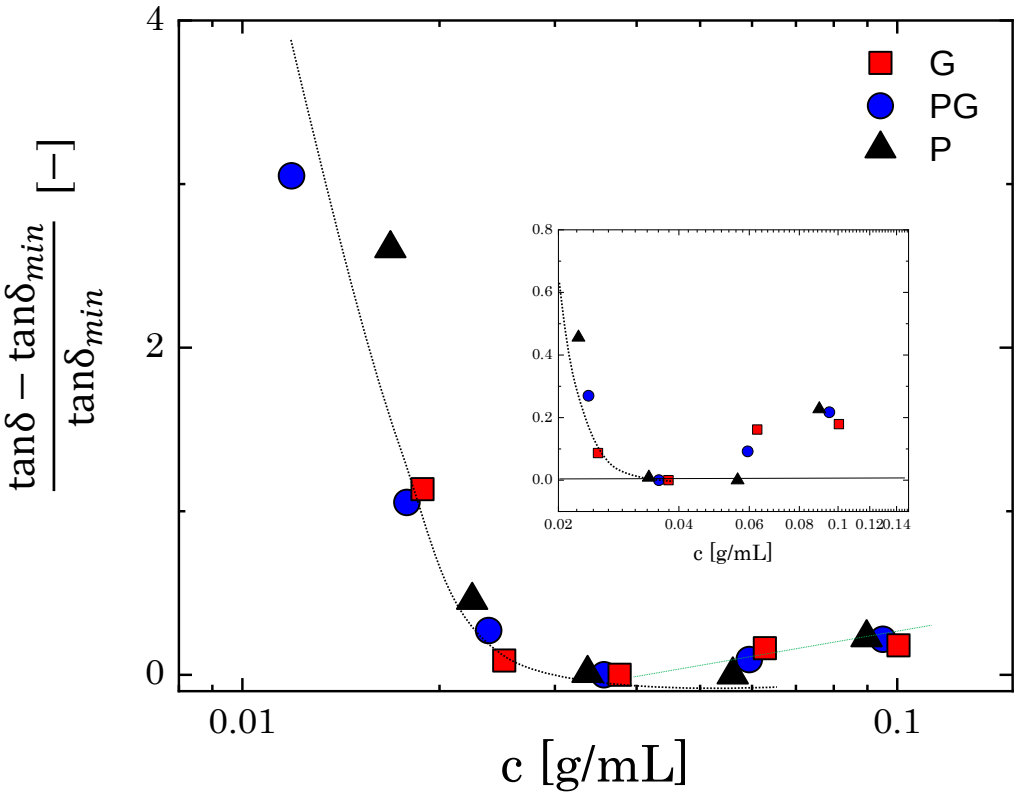

SI-4. 1: Evolution of the normalised loss tangent with Carbopol concentration at a fixed frequency ($\omega = 1$ Hz) for G, PG and P solutions. The inset zooms closer to the point where the loss tangent increases again. The dotted lines are guides for the eye.

SI-5 Graphical representation of the determination of the yield strain γ_y obtained from LAOS

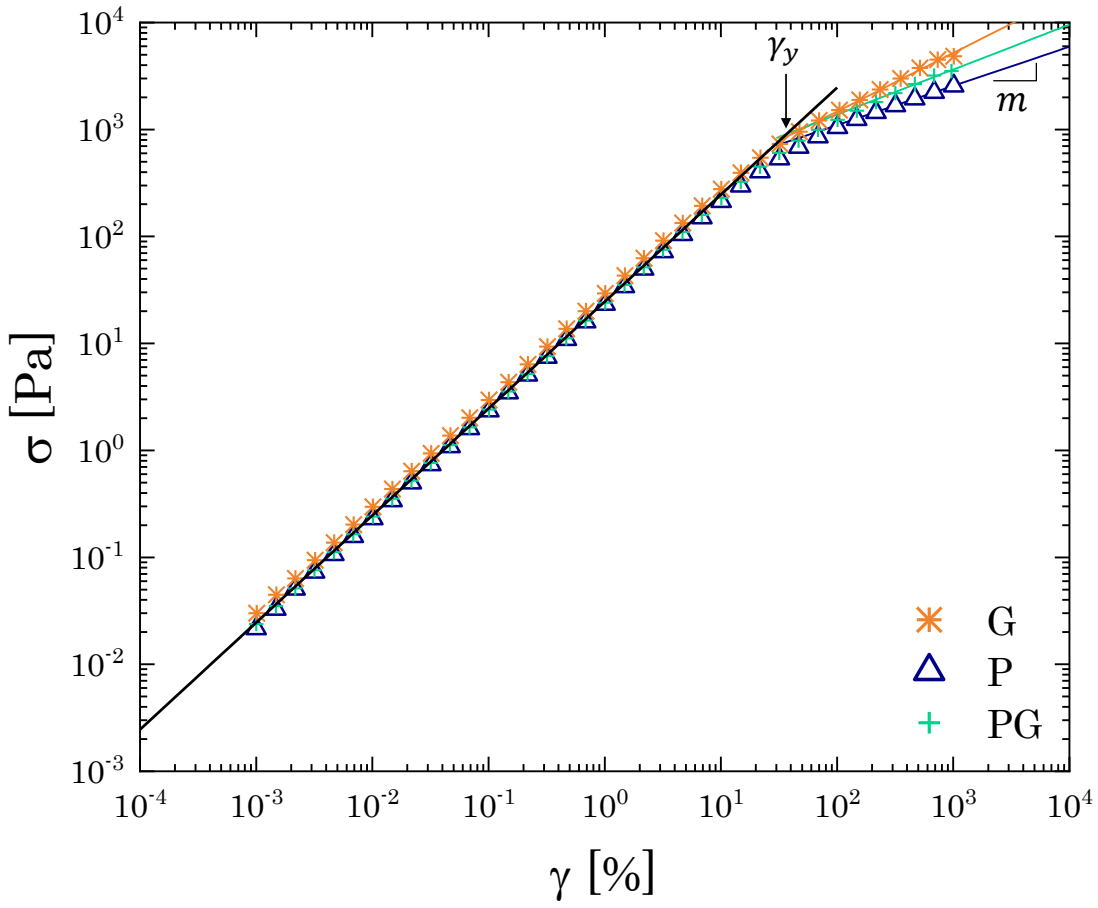

SI-5. 1: Shear stress (amplitude) vs shear strain (amplitude) at ω = 1 rad/s for 8% wt Carbopol samples obtained from LAOS experiments. The black line is the fitting for the linear regime, whilst the other lines are the power law fittings with slop m.

SI-6 Discrepancy between σ_y and σ_B as a function of Carbopol apparent volume fraction

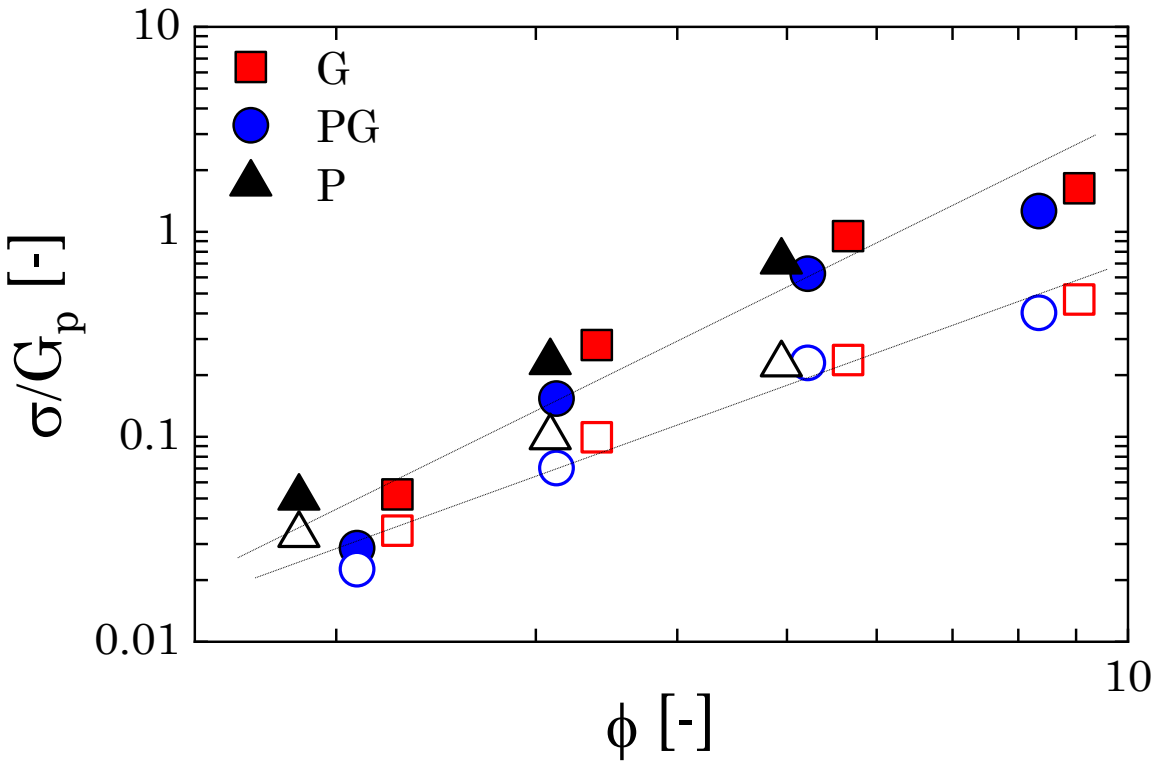

SI-6. 1: Discrepancy between σ_y (closed symbols) and σ_B (hollow symbols) as a function of Carbopol apparent volume fraction for G, PG and P solutions. The values reported are normalised with the particle modulus G_p reported in Table 4 of the main manuscript. The dotted lines are guides of the eye.

SI-7 Carreau-Yasuda fitting parameters

In the range of intermediate concentrations, between the dilute and glassy regimes, all dispersions present a shear-thinning behaviour that can be modelled with the Carreau-Yasuda equation:

$$\eta = \eta_\infty + (\eta_0 - \eta_\infty)(1 + (\dot{\gamma}\tau_0)^a)^{\frac{n_c-1}{a}} \qquad (SI\text{-}7.1)$$

where η is the shear viscosity obtained from the rheometer and corrected with the Weissenberg-Rabinowitsch correction, η_∞ is the infinite-shear viscosity, η_0 is the zero-shear viscosity, τ_0 is the Carreau relaxation time, which indicates the onset of the shear-thinning behavior, a is a fitting parameter, which is related to the smoothness of the transition between the zero-shear and the infinite-shear plateau, n_c is the flux index. Values of the parameters for each solvent can be found in the tables below.

SI-7. 2: Values of the fitting parameters of the Carreau-Yasuda model for G solutions

w_c (%)	η_∞ (Pa s)	η_0 (Pa s)	τ_0 (s)	n_c $(-)$	a $(-)$
0.15	0.815	1.03	0.078	0.81	0.5
0.2	0.835	1.29	0.1	0.76	0.5
0.4	0.965	2.81	0.57	0.75	0.25
0.5	0.98	6.86	1.35	0.72	0.2
0.55	1.07	20.5	10	0.66	0.25
0.6	1.2	44.2	82.2	0.65	0.25
0.7	1.5	61.7	141.5	0.65	0.25

SI-7. 3: Values of the fitting parameters of the Carreau-Yasuda model for PG solutions

w_c (%)	η_∞ (Pa s)	η_0 (Pa s)	τ_0 (s)	n_c $(-)$	a $(-)$
0.2	0.36	0.55	0.102	0.84	0.5
0.3	0.39	0.82	0.257	0.83	0.5
0.4	0.43	1.13	0.9	0.8	0.5
0.5	0.52	2.51	5.2	0.78	0.5
0.55	0.54	5.12	15.1	0.77	0.5
0.6	0.6	9.31	85.3	0.76	0.5
0.7	0.88	42.9	352	0.635	0.5

SI-7. 4: Values of the fitting parameters of the Carreau-Yasuda model for P solutions

w_c (%)	η_∞ (Pa s)	η_0 (Pa s)	τ_0 (s)	n_c $(-)$	a $(-)$
0.2	0.0935	0.125	0.01	0.99	0.5
0.4	0.095	0.192	0.05	0.9	0.9
0.5	0.098	0.235	0.1	0.89	0.5
0.7	0.102	0.394	0.35	0.89	0.9
0.8	0.105	0.812	0.98	0.845	0.9
1	0.15	2.77	22.5	0.78	0.9

SI-8 Reversibility of the yielding behavior near the jamming transition

Ascending and descending amplitude sweeps for G and PG solutions near the jamming transition (1.5% wt) are reported below (SI-5.1). The behaviour is the same observed for P solutions. The response to non-linear deformations is perfectly reversible for strain above γ_{c2}. At lower strains, the dispersions partially loose the initial structure, showing a decrease of the linear plateaus of G'' and G' obtained with the descending sweeps. However, the reduction is mild (i.e. for both solvents the reduction factor is of 1.2 and of 1.4, respectively for G'' and G').

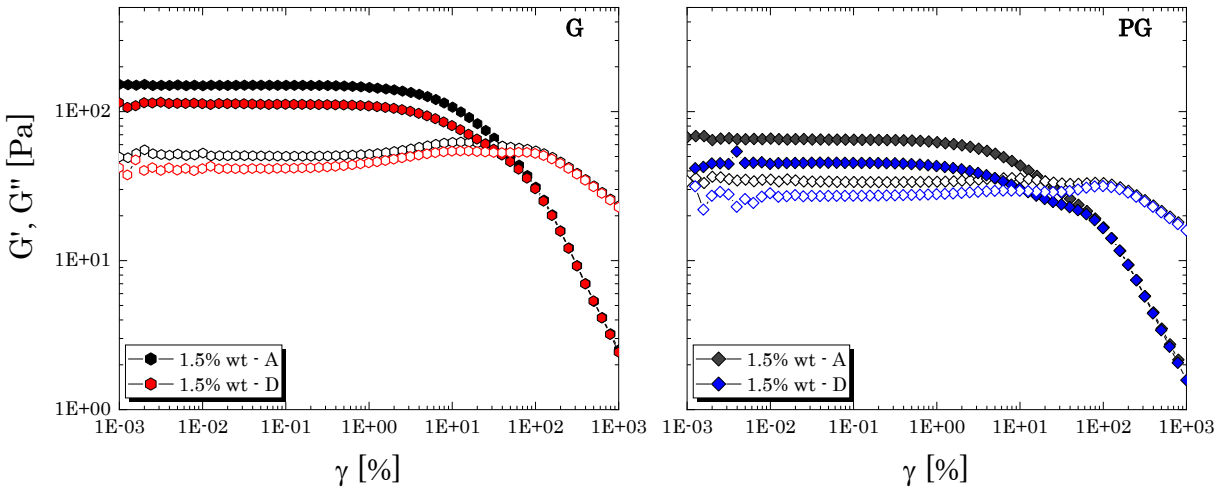

SI-8. 1: Ascending (A) and descending (D) amplitude sweeps for G solution (left) and PG solution (right) close the jamming transition. Closed symbols indicate the storage modulus, whilst hollow symbols the loss modulus.

SI-9 Determination of Mooney's equation parameters

In the hypothesis of a linear relation between the volume and the mass fraction of Carbopol particles in the most diluted regimes studied, the constant of proportionality k_M, can be found through the use of theoretical models for the relative viscosity of hard sphere suspensions. To this end, Mooney's equation for the viscosity of concentrated hard spheres suspensions was used. As shown in Eq.7 of the manuscript, in its original form, the equation contains one fitting parameter λ, which takes into account the effect of crowding that is strictly dependent from the polydispersity of the system. For perfectly monodisperse spheres, λ is equal to the reciprocal of the maximum packing achievable (i.e. $1.35 < \lambda < 1.91$). However, if the system is polydisperse, the parameter λ can assume values lower than 1.35, Mooney (1951). Therefore, assuming that the polydispersity of the dry Carbopol powder is maintained once it has swollen, the parameter λ should be the same for all samples studied and the two sets of data presented in Fig.11 can be treated as a vectorial set of data of the form:

$$\boldsymbol{y} = y_1\boldsymbol{i} + y_2\boldsymbol{j} \tag{SI-9.1}$$

where y_1 and y_2 are the set of experimental data for G and PG dispersions and P dispersions, respectively, which can then be fitted with the vectorial equation:

$$\boldsymbol{f_M} = f_1(\boldsymbol{x},\boldsymbol{\beta}) + f_2(\boldsymbol{x},\boldsymbol{\beta}) \rightarrow \boldsymbol{f_M} = \exp\left(\frac{2.5k_{M1}c}{1-\lambda k_{M1}c}\right) + \exp\left(\frac{2.5k_{M2}c}{1-\lambda k_{M2}c}\right) \tag{SI-9.2}$$

Hence, if the least squares method is used to obtain the optimal fitting parameters, the final equation to minimise is:

$$min\,\|\boldsymbol{y} - \boldsymbol{f_M}\| \rightarrow \min\left[\left(y_1 - \exp\left(\frac{2.5k_{M1}c}{1-\lambda k_{M1}c}\right)\right)^2 + \left(y_2 - \exp\left(\frac{2.5k_{M2}c}{1-\lambda k_{M2}c}\right)\right)^2\right] \tag{SI-9.3}$$

which yields the parameters presented in Table 4.

At this point, the data in Fig.11 can be replotted as a function of volume fraction (Fig.12 in the main manuscript).

References

M. Mooney, Journal of Colloid Science, 1951, **6**, 162–170.